Research Paper
J. Astron. Space Sci. 32(3), 181-187 (2015)
http://dx.doi.org/10.5140/JASS.2015.32.3.181

JASS Journal of Astronomy and Space Sciences

Storm Sudden Commencements Without Interplanetary Shocks

Wooyeon Park[1,2], Jeongwoo Lee[3,4], Yu Yi[1], Nicholas Ssessanga[5], Suyeon Oh[6†]

[1]Department of Astronomy, Space Science and Geology, Chungnam National University, Daejeon 34134, Korea
[2]Korea Astronomy and Space Science Institute, Daejeon 34055, Korea
[3]Center for Solar and Terrestrial Research, New Jersey Institute of Technology, Newark, NJ 07102, USA
[4]Astronomy Program, Department of Physics and Astronomy, Seoul National University, Seoul 08826, Korea
[5]South African National Space Agency (SANSA) Space Science, Hermanus 7200, South Africa
[6]Department of Earth Science Education, Chonnam National University, Gwangju 61186, Korea

Storm sudden commencements (SSCs) occur due to a rapid compression of the Earth's magnetic field. This is generally believed to be caused by interplanetary (IP) shocks, but with exceptions. In this paper we explore possible causes of SSCs other than IP shocks through a statistical study of geomagnetic storms using SYM-H data provided by the World Data Center for Geomagnetism – Kyoto and by applying a superposed epoch analysis to simultaneous solar wind parameters obtained with the Advanced Composition Explorer (ACE) satellite. We select a total of 274 geomagnetic storms with minimum SYM-H of less than –30nT during 1998-2008 and regard them as SSCs if SYM-H increases by more than 10 nT over 10 minutes. Under this criterion, we found 103 geomagnetic storms with both SSC and IP shocks and 28 storms with SSC not associated with IP shocks. Storms in the former group share the property that the strength of the interplanetary magnetic field (IMF), proton density and proton velocity increase together with SYM-H, implying the action of IP shocks. During the storms in the latter group, only the proton density rises with SYM-H. We find that the density increase is associated with either high speed streams (HSSs) or interplanetary coronal mass ejections (ICMEs), and suggest that HSSs and ICMEs may be alternative contributors to SSCs.

Keywords: geomagnetic storm, storm sudden commencement, SYM-H, interplanetary shock, high speed stream

1. INTRODUCTION

Geomagnetic storms are often preceded by a sudden increase of geomagnetic fields, a phenomenon termed storm sudden commencement (SSC). SSC storms occur as the magnetopause is compressed by interplanetary perturbations (Wilken et al. 1982; Tsurutani et al. 1995; Takeuchi et al. 2002). A dominant agent for such perturbations is believed to be interplanetary (IP) shocks. Indeed, many SSCs are accompanied by IP shocks, but with exceptions. Burlaga & Ogilvie (1969) found that all seven SSC events under their study were caused by IP shocks, but reported five IP shocks that were not followed by geomagnetic storms. Chao & Lepping (1974) studied SSCs that occurred during the solar maximum period of 1968-1971 and investigated 48 SSCs with full information on IMF and plasma data, finding that 41 were associated with interplanetary (IP) shocks. Smith et al. (1986) analyzed the data from ISEE 3 satellite and found that during the period of 1978 through 1979, about 75-90% of SSCs were related to IP shocks and 80% of IP shocks were related to SSCs and the others were related to sudden impulses. Wang et al. (2006) performed a statistical study on the SSCs and IP shocks during the period of 1995-2004. About 75% of the SSCs were found to be related to IP shocks. They also investigated effects of speed and direction of IP shocks on SSC rise times and found that the faster IP shocks, the shorter the rising time

Received May 27, 2015 **Revised** Jul 29, 2015 **Accepted** Aug 5, 2015
†**Corresponding Author**
E-mail: suyeonoh@jnu.ac.kr, ORCID: 0000-0002-6786-620X
Tel: +82-62-530-2517, Fax: +82-62-530-2519

of the SSC, and that significantly slanted IP shocks may lead to a delay in the rise of the SSC. Russell et al. (1992, 1994) have found that the square root of the dynamic pressure (P_{dyn}) of IP shocks has a high correlation with SSCs. They also found that the response differs according to the local time and the direction of the IMF. These studies indicated that IP shocks are the main contributor to SSCs.

We, however, note that not all SSCs are associated with IP shock as already indicated by the afore-mentioned statistical studies. For instance, the finding by Wang et al. (2006) that 75% of SSCs are related to IP shocks implies that there may be alternative drivers for SSCs for the remaining 25%. Correct identification of SSC drivers is important for understanding the dynamics of the Earth's magnetosphere. The relationship between the other geomagnetic activity indices and solar wind parameters has been studied (Oh 2013; Oh & Kim 2013; Kim & Chang 2014a, b). In this paper, we present a statistical study of geomagnetic storms focused on SSCs without IP shocks. We first sort out geomagnetic storms with SSCs that are not accompanied by IP shocks. We then compare their properties with those of SSCs accompanied by IP shocks, as determined using a superposed epoch analysis. From the distinct properties we hope to find clues to the possible cause of SSCs other than IP shocks.

2. DATA AND CLASSIFICATION

2.1 Data

The Disturbance Storm Time (Dst) index is generally used for identifying geomagnetic storms (Sugiura & Wilson 1964). In the present study, however, we use SYM-H (Iyemori 1990), which can also be used as a measure for geomagnetic field change (Wanliss & Showalter 2006). The main reason for choosing SYM-H is that it is given in units of minute while the Dst index is given in units of hour. The higher time cadence of SYM-H is essential for the present study because the increase of geomagnetic fields in SSC occurs in a timescale of tens of minutes. SYM-H used in this study was obtained from World Data Center for Geomagnetism – Kyoto (http://wdc.kugi.kyoto-u.ac.jp/aeasy/index.html).

We also obtain 1-minute average OMNI Web data of IMF magnitude (B), z-component (B_z), solar wind speed (V_p), and proton number density (N_p) in the solar wind from the Coordinated Data Analysis Web (CDAWeb) maintained by NASA's Goddard Space Flight Center (GFSC); OMNI Web data are the result of shifting the time of satellites data obtained at their orbits into those of about 10 R_E (the nose of the bow shock) (http://cdaweb.gsfc.nasa.gov/). To gather information of IP shocks we use the list of IP shocks toward the Earth based on Oh et al. (2007); Wang et al. (2010); and the ACE Lists of Disturbances and Transients prepared by ACE/MAG team (http://www.ssg.sr.unh.edu/mag/ace/ACElists/obs_list.html). To gather information on ICME and HSS, we used the list of ICMEs created by Ian Richardson and Hilary Cane (Near-Earth Interplanetary Coronal Mass Ejections since January 1996; http://www.srl.caltech.edu/ACE/ASC/DATA/level3/icmetable2.htm), the list of HSS associated with storms by O. Maris (COMPLEX CATALOGUE of GEOMAGNETIC STORMS-HIGH SPEED STREAMS; 1996 – 2008; http://www.spacescience.ro/new1/GS_HSS_Catalogue.htm), and the list of Stream Interaction Regions (SIRs) from Wind and ACE Data during 1995 – 2009 compiled by Jian et al. (2011) (http://www-ssc.igpp.ucla.edu/~jlan/ACE/Level3/SIR_List_from_Lan_Jian.pdf).

2.2 Typical Behaviors

Fig. 1 shows solar wind parameters and SYM-H for a geomagnetic storm that exhibits an SSC associated with IP shocks. From the top panel to the bottom panel, we show the interplanetary magnetic field strength, B, and its Geocentric Solar Magnetospheric (GSM) z-component, B_z (GSM), the solar wind velocity, V_p, and the proton number

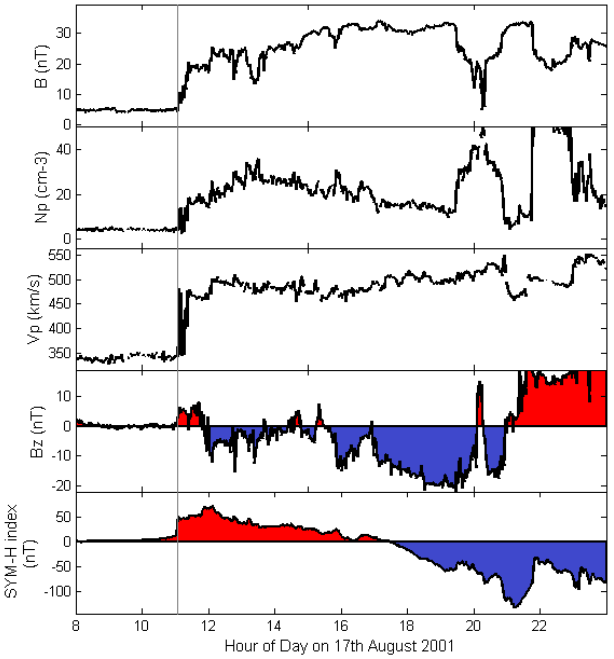

Fig. 1. Physical parameters of the geomagnetic storm on 17 August 2001 showing SSC accompanied by IP shocks. From the top to bottom panel, B, GSM B_z, V_p, N_p, and SYM-H are plotted as functions of time. The vertical guideline in all panels denotes the start time of SSC.

density, N_p, along with SYM-H. The three parameters: B, V_p, and N_p rapidly increase almost simultaneously at the time of SSC (denoted by the vertical guideline). The proton speed and density, V_p and N_p, evidently increase at the time of the SSC. The dynamic pressure of solar wind ($P_{dyn} \propto N_p \cdot V_p^2$) thus rapidly increases at the time of SSC and enhances the Earth's magnetic field. The GSM z-component of the IMF is another important factor for geomagnetic storms. Before SSC, B_z is nearly zero. At ~10 UT, B_z shows an abrupt change to become northward, and SYM-H rapidly increases, signaling the start of the SSC. After B_z turns to the southward direction, SYM-H gradually decreases. The direction of B_z shuffles between north and south for about five hours after SSC started, and then increases to southward until 19 UT and finally return to north at 20 UT.

Fig. 2 shows temporal variations of the parameters during a geomagnetic storm, revealing an SSC not accompanied by IP shocks. In this case, SYM-H is initially steady at ~10 nT and suddenly increases at ~02 UT AM by ΔSYM-H = 21 nT during 14 minutes. At the time of SSC (vertical grey guideline in Fig. 2), N_p abruptly increases and fluctuates for about an hour, which is a common feature for this type of SSC. However, B and V_p do not show as much variation as N_p. About 10 minutes earlier than the SSC, B_z rapidly drops from nearly zero to a negative value of about -20 nT and is sustained at this value until ~05 UT. During this period, SYM-H continues to decrease and the main phase of the geomagnetic storm follows.

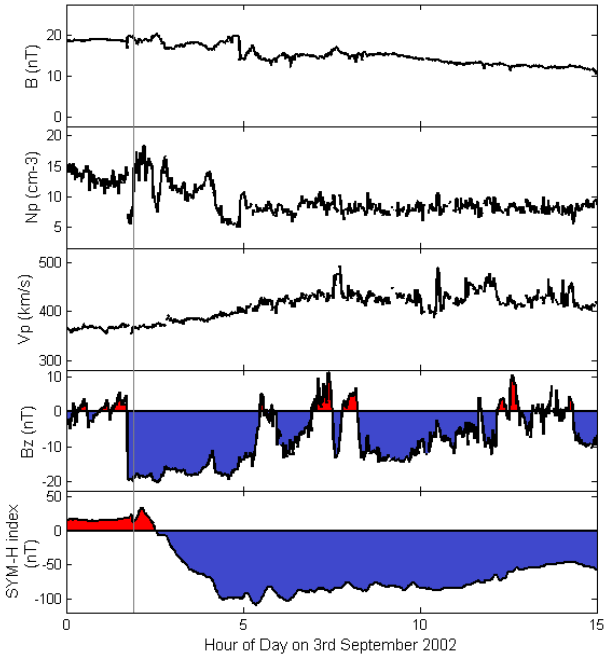

Fig. 2. Physical parameters of the geomagnetic storm on 3 September 2002 showing a SSC not accompanied by IP shocks. The parameters are displayed in the same format as Fig. 1.

To summarize, the time evolution of solar wind parameters around the SSC with IP shocks (Fig. 1) differs from that of the SSC without IP shocks (Fig. 2) in that all three parameters (B, V_p, N_p) simultaneously increase at the time of SSC in the former event and only N_p shows an obvious increase in the latter event. As another characteristic, B_z abruptly changes to the north direction at the SSC in the former event, while B_z rapidly drops to a negative value in the latter event.

2.3 Classification of Storms with SSC

Inspired by the above observation of two types of SSCs we examine a larger set of geomagnetic storms. During the period from 1998 to 2008, we select 407 storms with a minimum SYM-H of less than -30 nT. Usually SYM-H is near zero prior to geomagnetic storms, but for some strong events, the index can be negative even before the storms, which we include in the present study. However, we exclude 133 storms that are too weak to identify any SSCs. For the remaining 274 storms, we classify them into four groups according to the existence of SSC and IP shock. Group 1 comprises events with both SSC and IP shock and Group 2 consists of storms that do not have either an SSC or an IP shock. Storms of Group 3 have only SSC without IP shock and storms of Group 4 are associated with only IP shock without SSC.

We classify the SSCs under two different criteria in order to check the sensitivity of the resulting classification to the selection criteria. Our first criterion of SSC is that SYM-H should increase by more than 5 nT in 10 minutes prior to the beginning of the main phase (Kim et al. 2007). The results are shown in Table 1. Storms of Group 3 dominate (41%) and those of Group 1 are ranked second with a fraction of 39%. The fractions of the remaining groups are about 20%. While it is generally known that about 70-80% of SSCs are associated with IP shock, the number of SSCs that are not associated with IP shocks is higher than expected in this study. Only 49% of them (107 out of 220 SSCs) are associated with IP shock. However, only three storms are associated with IP shock but without SSC. The physical parameters of the IP shocks associated with these three storms show relatively smaller increases than those of other IP shocks.

In the second attempt, we modified the criterion of SSC such that SYM-H should increase by 10 nT in 10 minutes.

Table 1. Classification of geomagnetic storms under the SSC criterion No. 1 (ΔSYM-H >5 nT during 10 minutes).

	IP Shock Presence	IP Shock Absence
SSC Presence	Group 1: 107	Group 3: 113
SSC Absence	Group 4: 3	Group 2: 51

Table 2. Classification of geomagnetic storms under the SSC criterion No. 2 (ΔSYM-H >10 nT during 10 minutes).

	IP Shock Presence	IP Shock Absence
SSC Presence	Group 1: 103 (-114.5 nT)*	Group 3: 28 (-86.3 nT)
SSC Absence	Group 4: 7 (-57.7 nT)	Group 2: 136 (-57.9 nT)

*The numbers in the brackets represent the average minimum SYM-H for each group.

Under this criterion the number of Group 3 storms falls to 28 while that of Group 1 did not change substantially (Table 2). The total number of SSC storms is 131, 79% of which are associated with IP shocks. The results of the latter classification are similar to previous results (Smith et al. 1986; Wang et al. 2006). Since such a selection effect is not the primary goal of the present study, we finally set the criterion as ΔSYM-H >10 nT over 10 minutes for SSC and proceed to the next step of classification of SSCs.

Table 2 also lists the average minimum SYM-H for each group. The average magnitude of storms for Group 1 is the largest, followed by that for Group 3, even though IP shocks are absent. The storms in Groups 2 and 4 have relatively small magnitude of SYM-H regardless of whether IP shocks are present or not.

3. SUPERPOSED EPOCH ANALYSIS

In order to identify the behavior of physical parameters for Groups 1 and 3, we apply the superposed epoch analysis (O'Brien et al. 2001) to the physical parameters of our interest: SYM-H, N_p, B, and B_z. In this procedure, we set the reference time of each storm to the time of the maximum SYM-H of SSC, and then average each physical parameter for all storms for the time interval of two hours before and after the reference time. The results of this superposed epoch analysis for Groups 1 and 3 are shown in Fig. 3 with black and grey curves, respectively.

For Group 1 the solar wind parameters B, V_p, and N_p increase almost simultaneously with the increase of SYM-H while B_z stays nearly zero. For Group 3 storms, SYM-H does not rise as rapidly as Group 1 storms. SYM-H of Group 3 increases more slowly and decreases faster than that of Group 1. As additional different behaviors, the IMF strength, B, and the solar wind speed, V_p, increase but do not change as significantly as SYM-H. Only N_p exhibits a temporal variation similar to that of SYM-H. It thus appears that N_p is the parameter sensitive to SSC in Group 3, whereas B and V_p behave inconsistently with SYM-H. B_z of Group 3 also shows a different behavior from that of Group 1. It turns southward before SYM-H reaches its maximum.

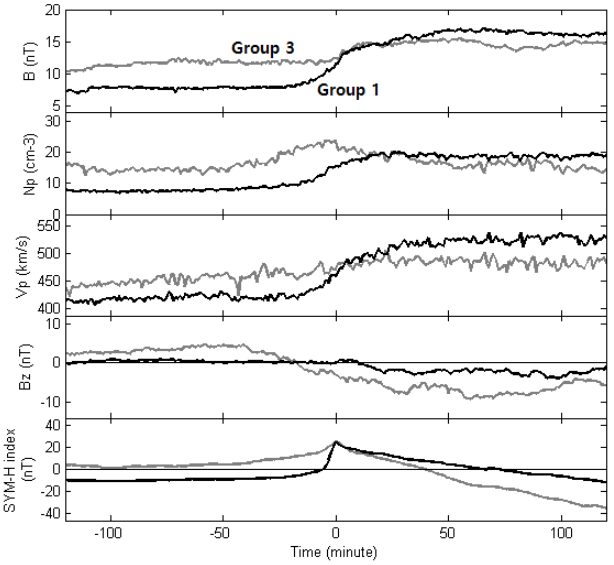

Fig. 3. Results of the superposed epoch analysis for Group 1 plotted in the same format as Fig. 1. From the top to bottom panel, B, GSM B_z, V_p, N_p, and SYM-H are plotted as functions of the relative time centered at the time of the maximum SYM-H. These parameters are averaged quantities for Group 1 (black curves) and Group 3 (grey curves), respectively.

4. FURTHER ANALYSIS OF GROUP 3 STORMS

4.1 Possible Sources

In Table 3 we list the physical parameters of Group 3, which consists of a total of 28 storms with SSCs defined by an increase of SYM-H by more than 10 nT within 10 minutes. The first four parameters are increments of magnetic field, proton velocity, number density, and dynamic pressure associated with SSCs, as obtained from ACE. The last column shows the source of SSCs, which we determine by referring to the list of ICMEs created by Ian Richardson and Hilary Cane (Near-Earth Interplanetary Coronal Mass Ejections Since January 1996), the list of HSS associated with storms by O. Maris (COMPLEX CATALOGUE of GEOMAGNETIC STORMS-HIGH SPEED STREAMS; 1996 – 2008), and the list of SIRs from Wind and ACE Data during 1995 – 2009 compiled by Jian et al. (2011). Since SIRs are generated by the interaction of relatively slow solar wind and HSS, we mark those events associated with SIR as HSS. Table 3 shows that the most common source for SSCs in Group 3 is HSS.

Fig. 4 summarizes the sources for SSCs in Group 3. HSS contributes to SSC in 21 events and ICME contributes to SSC in 10 events with an overlap between the two contributors. It is remarkable that 6 events are associated with both HSS and

Table 3. Increments of solar wind parameters and geomagnetic field during Group 3 storms.

Date (yyyymmdd)	ΔB (nT)	ΔVp (km/s)	ΔNp (cm^{-3})	ΔPdyn (nPa)	ΔSYM-H (nT)	Sources
19980504	20.46	169.6	8.75	3.05	54	ICME+HSS
19991022	2.23	42.1	12.33	4.74	27	HSS
20000516	1.61	39.7	1.77	3.1	11	ICME
20000523	8.35	26.3	36.16	27.34	40	ICME+HSS
20000915	3.63	33.6	14.59	5.25	14	
20001222						ICME
20010102	2.04	2.5	17.09	3.66	11	HSS
20010205	8.04	37.7	8.39	3.13	12	HSS
20010213	3.99	78.9	1.47	1.67	10	HSS
20010601	1.47	3.3	44.61	3.63	14	HSS
20010918	3.12	12.3	16.6	7.27	26	
20010923	12.61	20.9	4.94	3.02	19	ICME+HSS
20020904	0.35	2	10.43	3.19	21	HSS
20021217	0.61	10.1	19.76	6.33	30	ICME+HSS
20030226	-3.05	5.1	9.8	3.44	16	HSS
20030609	0.11	51.2	0.34	0.73	34	
20030716	0.22	23.7	0.43	0.81	11	HSS
20030909	0.63	14.5	3.09	1.36	14	HSS
20040309	3.43	16.3	10.74	4.62	20	HSS
20040403	5.23	39.5	15.63	6.59	20	ICME+HSS
20050107	2.52	14.8	14.4	8.14	16	ICME
20050116						ICME
20050529	0.67	23.5	17.68	9.91	48	ICME+HSS
20051227						HSS
20061109	3.89	20.1	20.29	6.85	13	HSS
20070720						HSS
20080325						HSS
20080404	1.38	16.7	4.75	2.48	15	HSS

(The blanks indicate the missing data.)

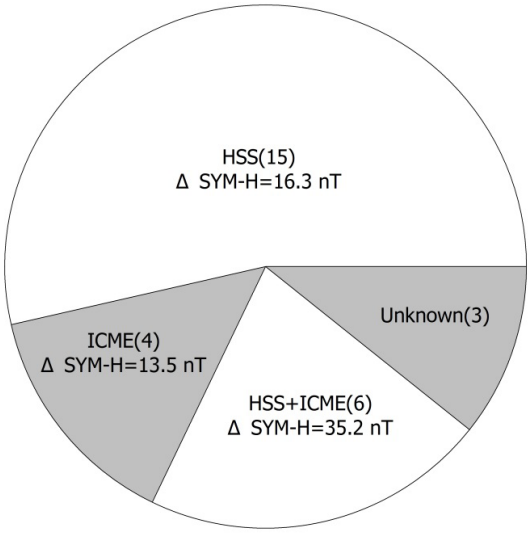

Fig. 4. Populations of Group 3 storms associated with HSS and ICME. Number of each subgroup and increment of SYM-H are also denoted.

ICME. These storms are associated with powerful solar wind and show a very large increase of SSC comparable to storms of Group 1 associated with powerful IP shock. As denoted in the figure, the storms associated with both HSS and ICME have a large increase of SYM-H of 35.3 nT on average. The storms with both ICME and HSS have a larger increase in physical parameters because HSS pushes ICME.

Our interpretation of the result is as follows: when HSS is the main contributor to SSC, N_p and B are observed to rapidly increase. We consider that, in this case, the interaction of HSS with the slowly moving solar wind compresses the plasma and magnetic field to result in SSCs although not as powerfully as IP shocks do. Because of magnetopause compression, N_p shows a rapid increase and then V_p increases slowly. When ICME is the main contributor to SSC, N_p and B of ICME are large and the resulting changes of parameters in the magnetopause are significant and consequently SSC can occur without IP shocks.

4.2 Comparison of Groups 1 and 3

Table 4. Average amount of parameter change during SSCs for Groups 1 and 3 storms.

	ΔB (nT)	ΔVp (km/s)	ΔNp (cm^{-3})	ΔSYM-H (nT)
Group 1	7.89	90.7	10.7	31.0
Group 3	3.63	30.6	12.8	21.6

We compare average physical parameters of Group 3 with those of Group 1 in Table 4. To obtain the average values, we selected only those storms for which complete data coverage is available: 64 storms from Group 1 and 23 storms from Group 3, respectively. For each event, the amount of increase in SYM-H and other physical parameters are determined from the interval of SSC.

Group 1 storms show changes of B, V_p, and SYM-H by large amounts in general. The amount of change of parameters during Group 1 storms is typically larger than that of Group 3 storms. ΔB and ΔV_p of Group 1 are two or three times larger than those of Group 3, and ΔSYM-H of Group 1 is 1.5 times larger than that of Group 3. In contrast, the average increase in N_p of Group 3 is 1.2 times larger than that of Group 1. In terms of N_p, Group 3 storms show a similar amount of change to Group 1 storms. The correlation coefficient between P_{dyn} and SYM-H is 0.77 for Group 1 and 0.40 for Group 3. It is likely that the compression of solar wind by HSS has a significant impact on the increase of N_p in Group 3.

5. SUMMARY

In this paper we have investigated whether IP shocks are essential for the occurrence of SSCs or some other drivers for SSCs operate. We analyzed 274 geomagnetic storms with a minimum SYM-H of less than –30 nT and changes of solar wind parameters associated with the storms. Selection of SSCs without IP shocks significantly depends on the criterion for SSC: more SSCs without IP shocks are found when weaker storms are included. Since such a selection effect is not the primary goal of the present study, we fixed the criterion of SSC to ΔSYM-H >10 nT over 10 minutes, under which the previous results by Wang et al. (2006) are closely reproduced. We then investigated the simultaneous interplanetary data and obtained the following results.

1. Of the 138 storms with either SSC or IP shocks, 75% are storms accompanied by both SSC and IP shocks (Group 1), 20% are SSCs without IP shocks (Group 3), and 5% are accompanied by IP shocks but without SSCs (Group 4). Additionally we found 136 storms with neither SSCs nor IP shocks (Group 2).

2. Our superposed epoch analysis shows that during Group 1 storms, temporal variations of solar wind parameters, B, V_p, and N_p, are similar to those of SYM-H. On the other hand, Group 3 storms show relatively slow temporal variations of B and V_p compared with those of SYM-H. Only the temporal change of N_p resembles that of SYM-H during Group 3 storms.

3. The GSM z-component of the IMF is another important factor for geomagnetic storms. For Group 1 storms, B_z becomes northward and turns to the south. SSC starts at the time of B_z being northward. For Group 3 storms, B_z changes from zero to the southward direction and the increases of N_p and SYM-H follow.

4. We further checked the association of Group 3 storms with HSS and ICME. We found that 21 of 28 storms result from HSS and 6 of those 21 storms result from HSS and ICME. The latter shows a larger increment of SYM-H.

5. For Group 1 storms, all parameters, B, V_p, and N_p, show obvious increases at the time of SSCs, which are known to be due to IP shocks. For Group 3 storms only N_p shows a distinct increment, and plausible sources for Group 3 should be able to compress the solar wind to enhance N_p without perturbing V_p.

Based on these results, we suggest that the interacting regions between HSS and slower solar wind stream ahead can also compress the magnetosphere to result in local enhancements of the proton number density and the IMF strength. The storms with both ICME and HSS show large increases in physical parameters because HSS pushes ICME. This could explain the aforementioned behaviors of SSCs that occur without IP shocks. IP shocks are therefore an important factor, but not a necessary condition, for SSCs.

ACKNOWLEDGEMENTS

This research was supported by the National Nuclear R&D Program through a National Research Foundation of Korea (NRF) grant funded by the Korea government (MSIP) (2014M2B2A9032253) and by the Space Core Technology Development Program through the Ministry of Education, Science and Technology (MEST) (2012M1A3A3A02033496). Also, this study was financially supported by Chonnam National University, 2014, and by Korea Polar Research Institute grants for Study of the upper and lower atmosphere coupling through 4-dimensional observations for the northern polar atmosphere: Polar upper atmospheric and space environmental changes (PE15090). JL was supported by the Brainpool Program of KOFST. JL is supported by

the BK21 Plus Program (21A20131111123) funded by the Ministry of Education (MOE, Korea) and National Research Foundation of Korea (NRF).

REFERENCES

Burlaga LF, Ogilvie KW, Causes of sudden commencements and sudden impulses, J. Geophys. Res. 74, 2815-2825 (1969). http://dx.doi.org/10.1029/JA074i011p02815

Chao JK, Lepping RP, A correlative study of SSC's, interplanetary shocks, and solar activity, J. Geophys. Res. 79, 1799-1807 (1974). http://dx.doi.org/10.1029/JA079i013p01799

Iyemori T, Storm-time magnetospheric currents inferred from mid-latitude geomagnetic field variations, J. Geomagn. Geoelectr. 42, 1249-1265 (1990). http://dx.doi.org/10.5636/jgg.42.1249

Jian LK, Russell CT, Luhmann JG, Comparing solar minimum 23/24 with historical solar wind records at 1 AU, Sol. Phys. 274, 321-344 (2011). http://dx.doi.org/ 10.1007/s11207-011-9737-2

Kim JH, Chang HY, Statistical Properties of Geomagnetic Activity Indices and Solar Wind Parameters, J. Astron. Space Sci. 31, 149-157 (2014a). http://dx.doi.org/10.5140/JASS.2014.31.2.149

Kim JH, Chang HY, Spectral Analysis of Geomagnetic Activity Indices and Solar Wind Parameters, J. Astron. Space Sci. 31, 159-167 (2014b). http://dx.doi.org/10.5140/JASS.2014.31.2.159

Kim KH, Moon YJ, Cho KS, Prediction of the 1-AU arrival times of CME-associated interplanetary shocks: Evaluation of an empirical interplanetary shock propagation model, J. Geophys. Res. 112, A05104 (2007). http://dx.doi.org/10.1029/2006JA011904

O'Brien TP, McPherron RL, Sornette D, Reeves GD, Friedel R, et al., Which magnetic storms produce relativistic electrons at geosynchronous orbit?, J. Geophys. Res. 106, 15533-15544 (2001). http://dx.doi.org/10.1029/2001JA000052

Oh S, Dependence of Quite Time Geomagnetic Activity Seasonal Variation on the Solar Polar Magnetic Polarity, J. Astron. Space Sci. 30, 43-48 (2013). http://dx.doi.org/10.5140/JASS.2013.30.1.043

Oh S, Kim B, Variation of Solar, Interplanetary and Geomagnetic Parameters during Solar Cycles 21-24, J. Astron. Space Sci. 30, 101-106 (2013). http://dx.doi.org/10.5140/JASS.2013.30.2.101

Oh SY, Yi Y, Kim YH, Solar cycle variation of the interplanetary forward shock drivers observed at 1AU, Sol. Phys. 245, 391-410 (2007). http://dx.doi.org/10.1007/s11207-007-9042-2

Russell CT, Ginskey M, Petrinec S, Le G, The effect of solar wind dynamic pressure changes on low and mid-latitude magnetic records, Geophys. Res. Lett. 19, 1227-1230 (1992). http://dx.doi.org/10.1029/92GL01161

Russell CT, Ginskey M, Angelopoulos V, Effect of sudden impulses on currents in the auroral ionosphere under northward interplanetary magnetic field conditions: A case study, J. Geophys. Res. 99, 17617-17622 (1994). http://dx.doi.org/10.1029/94JA01232

Smith EJ, Slavin JA, Zwickl RD, Bame SJ, Shocks and storm sudden commencements, in Solar Wind Magnetosphere Coupling, eds. Kamide Y, Slavin JA (Terra Scientific, Tokyo, 1986), 345-365.

Sugiura M, Wilson CR, Oscillation of the geomagnetic field lines and associated magnetic perturbations at conjugate points, J. Geophys. Res. 69, 1211-1216 (1964). http://dx.doi.org/10.1029/JZ069i007p01211

Takeuchi T, Russell CT, Araki T, Effect of the orientation of interplanetary shock on the geomagnetic sudden commencement, J. Geophys. Res. 107, 1423 (2002). http://dx.doi.org/10.1029/2002JA009597

Tsurutani BT, Gonzalez WD, Gonzalez ALC, Tang F, Arballo JK, et al., Interplanetary origin of geomagnetic activity in the declining phase of the solar cycle, J. Geophys. Res. 100, 21717-21734 (1995). http://dx.doi.org/10.1029/95JA01476

Wang C, Li CX, Huang ZH, Richardson JD, The effect of interplanetary shock strengths and orientations on storm sudden commencement rise times, Geophys. Res. Lett. 33, L14104 (2006). http://dx.doi.org/10.1029/2006GL025966

Wang C, Li H, Richardson JD, Kan JR, Interplanetary shock characteristics and associated geosynchronous magnetic field variations estimated from sudden impulses observed on the ground, J. Geophys. Res. 115, A09215 (2010). http://dx.doi.org/10.1029/2006GL025966

Wanliss JA, Showalter KM, High-resolution global storm index: Dst versus SYM-H, J. Geophys. Res. 111, A02202 (2006). http://dx.doi.org/10.1029/2005JA011034

Wilken B, Goertz CK, Baker DN, Higbie PR, Fritz TA, The SSC on July 29, 1977 and its propagation within the magnetosphere, J. Geophys. Res. 87, 5901-5910 (1982). http://dx.doi.org/ 0.1029/JA087iA08p05901